

Resonant coupling of Rayleigh waves through a narrow fluid channel causing extraordinary low acoustic transmission

Victor M. Garcia-Chocano

Wave Phenomena Group, Universidad Politècnica de València, Camino de Vera s/n, E-46022 Valencia, Spain

Nagaraj

Department of Physics, University of North Texas, 1155 Union Circle # 311427, Denton, Texas 76203

Tomàs Lòpez-Rios

Institut Nèel, CNRS and University Joseph Fourier, Boîte Postale 166, 38042 Grenoble Cedex 9, France

Lyudmila Gumen

Universidad Popular Autónoma del Estado de Puebla, 21 Sur # 1103, 72160 Puebla, Mexico

Josè Sànchez-Dehesa

Wave Phenomena Group, Universidad Politècnica de València, Camino de Vera s/n, E-46022 Valencia, Spain

Arkadii Krokhin^{a)}

Department of Physics, University of North Texas, 1155 Union Circle # 311427, Denton, Texas 76203

(Received 30 November 2011; revised 30 April 2012; accepted 7 May 2012)

Coupling of Rayleigh waves propagating along two metal surfaces separated by a narrow fluid channel is predicted and experimentally observed. Although the coupling through a fluid (water) is weak, a strong synchronization in propagation of Rayleigh waves even for the metals with sufficiently high elastic contrast (brass and aluminum) is observed. Dispersion equation for two polarizations of the coupled Rayleigh waves is derived and experimentally confirmed. Excitation of coupled Rayleigh waves in a channel of finite length leads to anomalously low transmission of acoustic energy at discrete set of resonant frequencies. This effect may find useful applications in the design of acoustic metamaterial screens and reflectors. © 2012 Acoustical Society of America. [<http://dx.doi.org/10.1121/1.4744939>]

PACS number(s): 43.35.Pt, 43.20.Ks, 43.20.Mv, 43.35.Bf [ANN]

Pages: 2807–2815

I. INTRODUCTION

Transmission of waves through a subwavelength hole or slit in a screen is one of the traditional problems in the theory of diffraction.^{1–4} In the classical approach the walls of the screen are assumed to be rigid, i.e., the propagating wave does not penetrate inside.^{5–8} “Softened” Dirichlet or Neumann boundary conditions for the diffracted field changes drastically the results for the transmission. In optics it leads to highly unusual transmission of light through metal films perforated with a periodic array of subwavelength holes.^{9,10} This effect is due to resonant excitation of surface plasmons on the screen surface with finite conductivity (not a perfect conductor). Acoustic counterpart of the effect of extraordinary transmission through a perforated metal plate has been recently reported.^{11–13} The resonant enhancement of zero-order transmission was attributed to the coupling between diffractive waves and the Fabry–Perot resonant modes inside the apertures. As it was demonstrated in Ref. 14 some fine details of this effect can be explained only if the metal plate is considered as elastic material and the contribution of surface modes is taken into account.

The role of surface modes in the transmission of energy (electromagnetic or acoustic) through narrow apertures is

emphasized by the fact that the excitation of surface waves may not only strongly enhance transmission through subwavelength aperture but also may suppress transmission of the incident wave. It is well-known that even weak dissipation at the frequency of surface plasmon resonance leads to suppression of light transmission through perforated metal films with thickness less than the skin-depth.¹⁵ Similar effect of suppression of specular reflection was predicted in layered superconductors due to resonant excitation of Josephson plasma waves.¹⁶ Suppression of transmission and also reflection is due to abnormal absorption of electromagnetic energy at the resonance.

Here we report the effect of strong acoustic attenuation of ultrasound through a subwavelength slit formed by plates of two different metals—brass and aluminum—immersed in water. Deep minima in sound transmission have been observed at the frequencies corresponding to resonant excitation of Rayleigh waves in a finite-length water channel. The observed level of suppression of acoustic energy exceeds by orders of magnitude the level of attenuation in pure water. Thus, this effect may find useful applications as a metamaterial screener of ultrasound.

Recently we reported the effect of anomalous strong suppression of sound transmission in a fluid channel formed by two *identical* metal plates and proposed the mechanism of absorption related to resonant excitation of coupled

^{a)}Author to whom correspondence should be addressed. Electronic mail: arkady@unt.edu

Rayleigh waves.¹⁷ Coupling between the Rayleigh waves is weak since it is proportional to the ratio of the density of water to the density of metal. For identical metals such weak coupling is manifested as splitting of two degenerate Rayleigh waves into two channel eigenmodes with different polarization (symmetric and anti-symmetric) and slightly different phase velocities.¹⁸ At normal incidence only the symmetric mode is excited, therefore the characteristics of this mode only have been reported. In the present case of two different metals the coupling between the Rayleigh waves, which is still weak, leads to *strong* renormalization of the velocity of each Rayleigh wave. Due to synchronization in propagation of the Rayleigh waves the dispersion of two coupled modes becomes nonlinear. In this case the phase velocities of two channel eigenmodes lie between the velocities of the Rayleigh wave in brass and aluminum.¹⁹ As a result, we observed the minima corresponding to excitation of two eigenmodes (which are neither symmetric nor anti-symmetric) but not the resonances corresponding to excitation of the Rayleigh wave in brass and in aluminum separately.

Eigenmodes of a fluid channel clad between two solids have been considered in many previous publications. The problem was formulated by Lloyd and Redwood¹⁸ for an infinitely long channel formed by two solid plates of finite width. It was shown that coupled vibrations of the plates and water give rise to extremely low-frequency dispersive eigenmodes. At high frequencies it coincides with Stoneley–Scholte mode. This low-frequency guided mode was experimentally observed and its strong dispersion was measured.²⁰ Coupling between the Rayleigh modes in a solid-liquid-solid waveguide was studied in Refs. 19 and 21. A dispersion equation was derived in approximation of infinite waveguide channel in Ref. 19 and dispersion characteristics of the coupled Rayleigh modes have been measured using quartz delay line at ultrasound frequency of 30 MHz. Approximation of geometrical acoustics and good agreement between the theory and experiment was reported in Ref. 21 for high-frequency sound excitation. Both, symmetric and asymmetric trilayers were studied. Acoustic transmission and Lamb-mode coupling through ultra-thin fluid layer were reported in Ref. 22.

In all previous studies the length of the fluid channel was practically infinite, i.e., the resonant effect at the frequencies obtained from quantization of eigenmodes in a finite-length channel could not be observed. In the following we report the experimental results on acoustic transmission, derive the dispersion equation for the coupled Rayleigh waves and obtain the set of resonant frequencies for each eigenmode. We also predict and measure an interesting cut-off effect for one of the eigenmodes at apertures smaller than some critical value. It is commonly believed that longitudinal acoustic wave propagates freely through any narrow aperture (unlike transverse electromagnetic wave). This conclusion is based on numerous results obtained for rigid screens, see, e.g., Refs. 5 and 23. If, however, the vibrations of the surface of the slit (or hole) are taken into account, the propagating sound wave is not pure longitudinal. For one of the two eigenmodes (so-called fast mode with quasi-symmetric polarization) vibrations in the transverse direction prevent free propagation below some critically narrow aperture (or below some critical frequency at fixed aperture).

Recently a nonresonant acoustic metamaterial possessing double negative effective constitutive parameters has been proposed and numerically evaluated in Ref. 24. Unlike previous examples of acoustic metamaterials, the unit cell of this one does not contain resonant cavities. Instead, strong modification of the index of refraction is achieved by increase of the acoustic path length within a unit cell when sound propagates along a zigzag waveguide. Each segment of the waveguide is a fluid channel formed by two metal plates. Clear understanding of sound transmission through such fluid channels is, thus, directly related to design of nonresonant acoustic metamaterials. In particular, the cutoff of sound propagation through the channel that we predict and observe here (and in Ref. 17 for identical metals) may seriously modify the values²⁴ of the effective parameters of the metamaterial at very low frequencies.

II. EXPERIMENTAL SETUP AND RESULTS ON ACOUSTIC TRANSMISSION

The experiment is performed in a water bath of size $50 \times 60 \times 12 \text{ cm}^3$. The setup consists of two 1.5 in. immersion (V392-SU, Panametrics) transducers that are placed face to face separated by a distance of 16 cm. Slits are obtained between two adjacent but different metal plates (of dimension $12 \times 12 \text{ cm}^2$)—one of aluminum and one of brass—of equal thickness h . The slit is aligned and centered midway between both transducers while maintaining its aperture d with the help of a sample holder that fixes both metal plates by their upper part. The experimental setup is schematically shown in Fig. 1.

The emitter transducer is connected to a waveform generator Agilent 33220A, while the receiver transducer is connected to a digital oscilloscope NI PXI-5105. Prior to placing the sample, a direct measure between both transducers is performed. These data are then used as reference to normalize the subsequent measures, thus compensating the non-flat frequency response of the piezoelectric transducers. The last cycles of the received signal until the arrival of the first unwanted echo are selected to be processed by a sine fitting algorithm. This procedure ensures an echo free measurement. In order to ensure that the response corresponds to the steady state of the system, it is also important

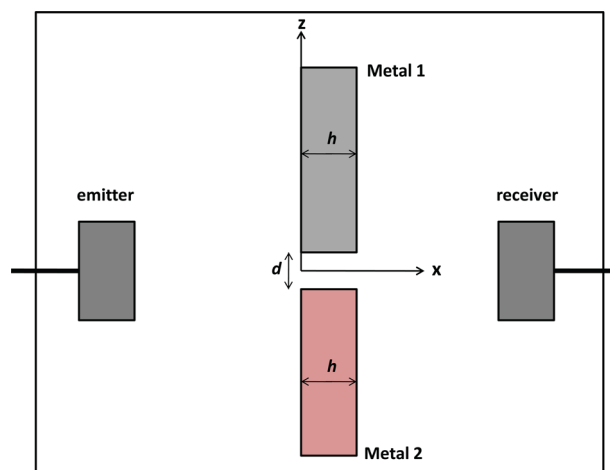


FIG. 1. (Color online) Experimental setup showing the geometrical parameters of the aperture (d) and length (h) of the slit.

to make sure that the envelope of the signal remains constant within the region where the cycles to be analyzed are extracted.

First, we measured sound transmission through square metal plates without the slit. It is well known that the metal-water interface reflects most of the incident acoustic energy at normal incidence, which implies that away from Fabry–Perot resonances the plates are practically opaque to sound. For the metal plates of finite thickness h , the resonant maximum occur when $\lambda_l = 2h/n$, where $n = 1, 2, 3, \dots$ and $\lambda_l = c_l/f_n$ is the wavelength of the longitudinal wave of linear frequency f_n .

In the experiments, the maxima in the transmission are situated exactly at Fabry–Perot resonances, which can be seen in Fig. 2 where the transmission spectra of the water channel with a fixed length h and different apertures d are plotted. The spectra in Fig. 2 also exhibit sharp minima indicating presence of sound absorption mechanism. Relevance of these resonances to excitation of the metal plates follows from simple relation giving the positions of absorption dips:

$$\lambda_{R_c} = c_{R_c}/f_n = 2h/n, \quad (1)$$

where n is an integer, λ_{R_c} and c_{R_c} are the wavelength and phase velocity of the eigenmode which is formed in the channel due to coupling between the Rayleigh waves propagating in the metal plates. This phase velocity is calculated below for from the dispersion equation for the coupled Rayleigh waves.

When the aforementioned condition is satisfied, the frequency of incident sound wave matches with one of the eigenfrequencies of the water channel clad between elastic surfaces. As a result, the amplitude of vibrations of the surfaces reaches a maximum. The acoustic energy penetrates into the metal plates more efficiently, giving rise to the minima in the transmission spectra. To calculate the positions of the

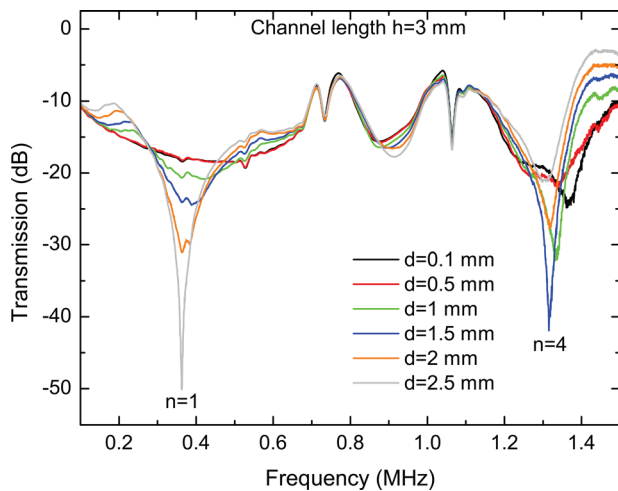


FIG. 2. (Color online) Transmission spectra obtained for several apertures d of the slit separating two water-immersed unidentical (brass and aluminum) metal plates for a channel length $h = 3$ mm. The maxima in the transmission are Fabry–Perot resonances. The minima are the frequencies where extraordinary absorption of sound occurs, corresponding to the frequencies of resonant excitation of coupled Rayleigh waves. Two resonances with $n = 1$ and $n = 4$ fall within the shown range of sound frequencies.

minima from Eq. (1) we need to know the dispersion relation for the propagating eigenmode.

III. DISPERSION EQUATION

An acoustic signal in the form of an ultrasonic plane wave impinged on the channel generates surface elastic (Rayleigh) waves, which would propagate independently and with different phase velocities if there would be no interaction between them through the fluid. Due to this interaction the propagation of two Rayleigh waves at the both sides and the sound wave in the fluid channel is synchronized. The wave that propagates in the whole system—metal plates and fluid channel—has a phase velocity, polarization, and dispersion which are calculated from the corresponding eigenvalue problem. The eigenvalue problem consists of two wave equations in elastic metals, one wave equation for sound in the fluid and the boundary conditions at the interfaces. In this section we derive the dispersion equation following a standard procedure, see, e.g., Refs. 18 and 25.

The displacement of the metal plates in terms of velocity potentials can be expressed as $\mathbf{w} = \nabla\xi + \nabla \times \mathbf{a}$ for metal 1 ($z > d/2$) and $\mathbf{u} = \nabla\phi + \nabla \times \mathbf{b}$ for metal 2 ($z < d/2$), where $\mathbf{a} = (0, a, 0)$ and $\mathbf{b} = (0, b, 0)$, see Fig. 1. The gradient and curl components of the displacement vectors correspond to longitudinal and transverse waves respectively, and satisfy the conditions that the divergence of transverse component and the curl of longitudinal component vanish.

The components of the velocity potentials are obtained from four wave equations

$$\nabla^2 a + \frac{\omega^2}{c_{1t}^2} a = 0, \quad (2)$$

$$\nabla^2 \xi + \frac{\omega^2}{c_{1l}^2} \xi = 0 \quad (3)$$

for metal 1 ($z > d/2$), and

$$\nabla^2 b + \frac{\omega^2}{c_{2t}^2} b = 0, \quad (4)$$

$$\nabla^2 \phi + \frac{\omega^2}{c_{2l}^2} \phi = 0 \quad (5)$$

for metal 2 ($z < d/2$). Here (c_{1t}, c_{1l}) and (c_{2t}, c_{2l}) are shear and compressional velocities (which we assume to be real) in metal 1 and metal 2, respectively. We are looking for the solutions of these equations in the form of plane waves propagating along axis x and evanescent waves away from the channel along axis z :

$$\begin{aligned} \phi(x, z) &= e^{Pz - i\omega t} (A_1 e^{iqx} + B_1 e^{-iqx}), \quad P = \sqrt{q^2 - \omega^2/C_{2l}^2}, \\ \xi(x, z) &= e^{-Qz - i\omega t} (A_2 e^{iqx} + B_2 e^{-iqx}), \quad Q = \sqrt{q^2 - \omega^2/C_{1l}^2}, \\ b(x, z) &= e^{Rz - i\omega t} (C_1 e^{iqx} + D_1 e^{-iqx}), \quad R = \sqrt{q^2 - \omega^2/C_{2t}^2}, \\ a(x, z) &= e^{-Sz - i\omega t} (C_2 e^{iqx} + D_2 e^{-iqx}), \quad S = \sqrt{q^2 - \omega^2/C_{1t}^2}. \end{aligned} \quad (6)$$

The dynamical equation for the velocity potential $\beta(x, z)$ in the fluid channel ($-d/2 < z < d/2$) is given by $\nabla^2 \beta + \omega^2/c_f^2 \beta = 0$, where c_f is the compressional wave velocity in water. The solution for $\beta(x, z)$ is a pure plane wave with components of the wave vector along axes x and z ,

$$\begin{aligned} \beta(x, z) &= e^{-i\omega t} [e^{i\kappa z} (K_1 e^{iqx} + L_1 e^{-iqx}) \\ &\quad + e^{-i\kappa z} (K_2 e^{iqx} + L_2 e^{-iqx})], \\ \kappa &= \sqrt{(\omega/c_f)^2 - q^2}. \end{aligned} \quad (7)$$

The oscillating pressure produced by sound wave in the fluid is obtained from the continuity equation

$$\rho_f \frac{\partial \mathbf{v}}{\partial t} + \nabla p' = 0, \quad (8)$$

where $\mathbf{v}(x, z) = \nabla \beta(x, z)$.

Solutions (6) and (7) of the wave equations in three different media are coupled through the boundary conditions at $z = \pm d/2$. At these interfaces the normal and shear stresses are continuous

$$\sigma_{zz} \left(z = \pm \frac{d}{2} \right) = -p' \left(z = \pm \frac{d}{2} \right), \quad \sigma_{xz} \left(z = \pm \frac{d}{2} \right) = 0, \quad (9)$$

and the normal components of the velocity are continuous

$$v_z = \frac{\partial \beta}{\partial z} \Big|_{z=+d/2} = \dot{w}_z = -i\omega w_z \left(z = \frac{d}{2} \right), \quad (10)$$

$$v_z = \frac{\partial \beta}{\partial z} \Big|_{z=-d/2} = \dot{u}_z = -i\omega u_z \left(z = -\frac{d}{2} \right). \quad (11)$$

Thus, these boundary conditions give 6 linear relations for 12 unknown constants in Eqs. (6) and (7). However, the unknown constants for the wave propagating to the right and the constants for the wave propagating to the left form two independent groups and can be considered separately. For each group there are six homogeneous equations for six unknowns. Equating the corresponding determinant to zero, we obtain, after some cumbersome algebra, the following dispersion relation between ω and q :

$$\tan \left(\frac{\kappa d}{2} \right) = \frac{(AB - CD) \pm \sqrt{(A^2 + C^2)(B^2 + D^2)}}{AD + BC}, \quad (12)$$

where A, B, C , and D are functions of ω and q given by

$$\begin{aligned} A &= (S^2 + q^2)^2 - 4SQq^2, \\ B &= (R^2 + q^2)^2 - 4RPq^2, \\ C &= \left(\frac{\rho_f \omega^2}{\rho_1 c_{1l}^2 \kappa} \right) Q(S^2 - q^2), \\ D &= \left(\frac{\rho_f \omega^2}{\rho_2 c_{2l}^2 \kappa} \right) P(R^2 - q^2). \end{aligned} \quad (13)$$

Here ρ_1, ρ_2 , and ρ_f are the densities of the metals and the fluid, respectively.

Relation (12) defines two eigenmodes, ‘‘plus’’ and ‘‘minus.’’ They have different polarizations and propagate with different phase velocities. We refer to them as ‘‘slow’’ and ‘‘fast’’ modes since the plus mode has lower phase velocity. If the channel is empty, $\rho_f = 0$, then $C = D = 0$ and Eq. (12) is reduced to two equations $A = 0$ and $B = 0$ which give the linear dispersion relations for the Rayleigh waves in metal 1 and metal 2, respectively. Solutions for independently propagating Rayleigh modes are shown in Fig. 3.

The coupling between the Rayleigh waves occurs when the parameters ρ_f/ρ_1 and ρ_f/ρ_2 are different from zero. This coupling leads to nonlinear dispersion of the channel eigenmodes. For a fluid channel clad between two identical metals Eq. (12) is reduced to two dispersion equations obtained in Ref. 17. In this particular case, the slow and fast modes become the modes with antisymmetric and symmetric polarization, respectively.

IV. SPECTRUM OF RESONANT FREQUENCIES

The dispersion relation Eq. (12) was obtained for an infinite channel where ω changes continuously with the wave vector q . In a finite-length channel this relation is not valid for all wave vectors. Resonant frequencies should be obtained from a complete solution for sound wave passing through the dissipative inhomogeneous metal-fluid-metal medium. Of course, this problem could not be solved analytically. We, however, found an approximate solution (which is in a good agreement with the experiment and numerical simulations) by quantizing the wave vector. The quantized values of q are obtained from the boundary conditions at the ends of the channel, $x = 0$ and $x = h$. Here the acoustic energy which is concentrated in a narrow channel enters into infinite fluid medium. The oscillating part of pressure $p(x, z)$ is strongly reduced within a narrow transition layer at the channel openings. Then, an approximate boundary condition can be written as follows:²⁶

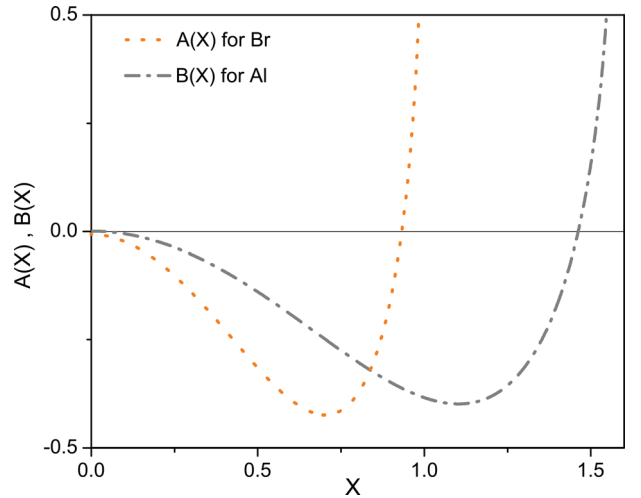


FIG. 3. (Color online) Plots of the functions $A(X)$ and $B(X)$ [see Eq. (13)] vs dimensionless parameter $X = \omega/qc_{1l}$. Normalized phase velocity for uncoupled Rayleigh wave in the absence of fluid in the channel ($C = D = 0$) for brass (aluminum) is given by the root $X = X_R$ of the dispersion equation $A(X) = 0$ [$B(X) = 0$]. The roots obtained from the graph are $X_{R_{Br}} = 0.936$ and $X_{R_{Al}} = 1.456$, respectively. The phase velocity of uncoupled Rayleigh wave $c_R = X_R c_{1l}$ for brass is $c_{R_{Br}} = 1.87$ km/s ($< c_{1l} = 1.997$ km/s) and for aluminum is $c_{R_{Al}} = 2.9$ km/s ($< c_{2l} = 3.13$ km/s).

$$p(x = 0, z) = p(x = h, z) = 0. \quad (14)$$

This equation is widely used in calculation of the resonant frequencies of pipes open at both ends. It ignores the presence of the transition layer. The corresponding correction grows with the widths of the pipe, therefore Eq. (14) becomes invalid for wide apertures. There are more limitations related to this approximation which we discuss in Sec. V.

Equation (14) together with Eq. (7) for the potential β and relation (8) gives that the wave vector takes only discrete values, $q_n h = \pi n$, $n = 1, 2, 3, \dots$. The eigenfrequencies $f_n = \omega_n / 2\pi$ of the channel can be written in the form $f_n = qc_{1l} X / 2\pi$, which is equivalent to Eq. (1). Substitution of this frequency into dispersion equation (12) leads to two equations (with plus and minus signs) for the dimensionless unknown parameter X (for each integer n).

In the special case when the metal plates on both sides of the fluid channel are identical, the incident acoustic wave propagating parallel to the axis of the channel excites only the symmetric mode.¹⁷ However, for the general case when the metal plates on both sides of the fluid channel are not identical, both slow and fast modes are excited though the excitation of the fast mode is relatively more pronounced. It is now convenient to express Eq. (12) in terms of unknown X :

$$F_{\pm}(X) = \frac{(AB - CD) \pm \sqrt{(A^2 + C^2)(B^2 + D^2)}}{(AD + BC) \tan\left(\frac{\kappa d}{2}\right)} = 1, \quad (15)$$

where A , B , C , D , and κ are transformed functions of X given by

$$\begin{aligned} A(X) &= q^4 \left[(2 - X^2)^2 - 4(1 - X^2)^{1/2} \left(1 - \frac{c_{1l}^2}{c_{1f}^2} X^2 \right)^{1/2} \right], \\ B(X) &= q^4 \left[\left(2 - \frac{c_{1l}^2}{c_{2f}^2} X^2 \right)^2 - 4 \left(1 - \frac{c_{1l}^2}{c_{2f}^2} X^2 \right)^{1/2} \right. \\ &\quad \left. \times \left(1 - \frac{c_{1l}^2}{c_{2f}^2} X^2 \right)^{1/2} \right], \\ C(X) &= -q^4 \left(\frac{\rho_f}{\rho_1} \right) \frac{\left(1 - \frac{c_{1l}^2}{c_{1f}^2} X^2 \right)^{1/2}}{\left(\frac{c_{1l}^2}{c_{1f}^2} X^2 - 1 \right)^{1/2}}, \\ D(X) &= -q^4 \left(\frac{\rho_f}{\rho_2} \right) \left(\frac{c_{1l}}{c_{2f}} \right)^4 \frac{\left(1 - \frac{c_{1l}^2}{c_{2f}^2} X^2 \right)^{1/2}}{\left(\frac{c_{1l}^2}{c_{2f}^2} X^2 - 1 \right)^{1/2}}, \\ \kappa(X) &= q \left(\frac{c_{1l}^2}{c_{2f}^2} X^2 - 1 \right)^{1/2}, \end{aligned} \quad (16)$$

where $q = q_n = n\pi/h$ and $X = 2\pi f_n / qc_{1l}$.

The solutions for X in $F_{\pm}(X)$ are obtained when $F_{\pm}(X) = 1$ (see Fig. 4). Hence the solutions for $F_+(X) = 1$ and

$F_-(X) = 1$ are denoted by X_+ and X_- , respectively. It is clear from Fig. 4 that for a given aspect ratio d/h that $F_-(X) > F_+(X)$. Since the velocity of coupled Rayleigh wave is proportional to the root X , it is appropriate to label $F_+(X)$ as the slow mode and $F_-(X)$ as the fast mode. Therefore, the phase velocities of coupled Rayleigh wave for the fast and slow modes are $c_{Rc}^- = c_{1l} X_-$ and $c_{Rc}^+ = c_{1l} X_+$, respectively.

The equations for $\kappa(X)$, $A(X)$, and $B(X)$ impose a strict condition that the real solutions corresponding to coupled Rayleigh waves described by Eq. (15) must fall within the interval $c_f / c_{1l} < X < 1$.²⁷ This means the velocity of coupled Rayleigh mode $c_{Rc} = X c_{1l}$ cannot exceed the shear velocity c_{1l} . Otherwise, when $c_{Rc} > c_{1l}$ the coupled mode becomes a leaky Rayleigh mode and radiates part of its energy into the metal with the corresponding shear velocity c_{1l} . In that case, the solutions for $F_{\pm}(X) = 1$ become complex: X_{LR} takes the form $X_{LR} = X'_{LR} + iX''_{LR}$, where the imaginary part X''_{LR} characterizes the attenuation length, which gives the depth and width of the resonant minimum. Further theoretical study on leaky Rayleigh waves radiating from metal-liquid interface can be found in Refs. 25, 28, and 29. Strong attenuation of Rayleigh waves has been recorded in a seismic study.³⁰ Rayleigh waves leaking into fluid from metal-fluid interface have also been experimentally studied.³¹

V. CORRESPONDENCE BETWEEN THEORY AND EXPERIMENT

The resonant frequency f_n scales as $1/h$ with the channel length. This is the same geometrical factor that defines also the Fabry–Perot resonances. There is, however, much weaker dependence of f_n on the channel aspect ratio d/h which enters through X . This dependence is shown in Fig. 5 for both eigenmodes and for resonances $n = 1$ and $n = 4$. It is clear that there is a tendency for the root X , corresponding to the fast mode to approach the critical value $X = 1$ as d/h decreases. Substituting $X = 1$ into equation $F_-(X) = 1$, we

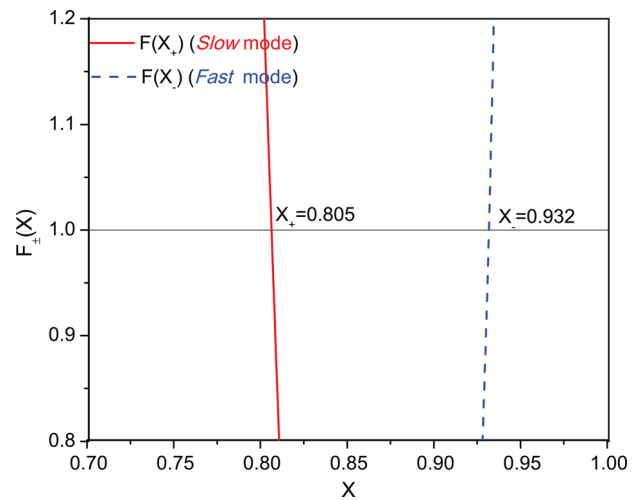


FIG. 4. (Color online) A typical plot showing the roots of the dispersion equations $F_{\pm}(X) = 1$ for slow and fast modes for $n = 4$, channel length $h = 3$ mm, and aperture $d = 4.5$ mm. $F_{\pm}(X)$ are related to the slow and fast modes. The plot is obtained for a metal combination of brass ($c_{1l} = 1.997$ km/s, $c_{1l} = 4.25$ km/s, $\rho_1 = 8.5$ gm/cm³) and aluminum ($c_{2l} = 3.13$ km/s, $c_{2l} = 6.32$ km/s, $\rho_2 = 2.7$ gm/cm³). The compressional velocity of sound in fluid (water) in the channel is taken as $c_f = 1.48$ km/s.

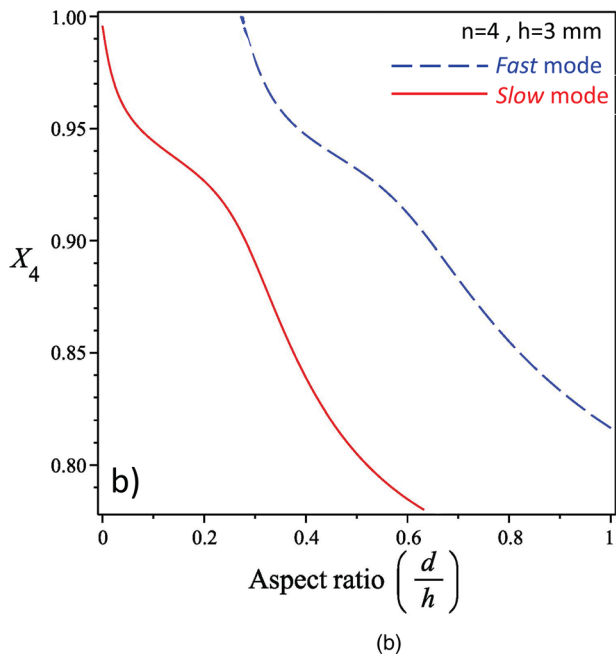
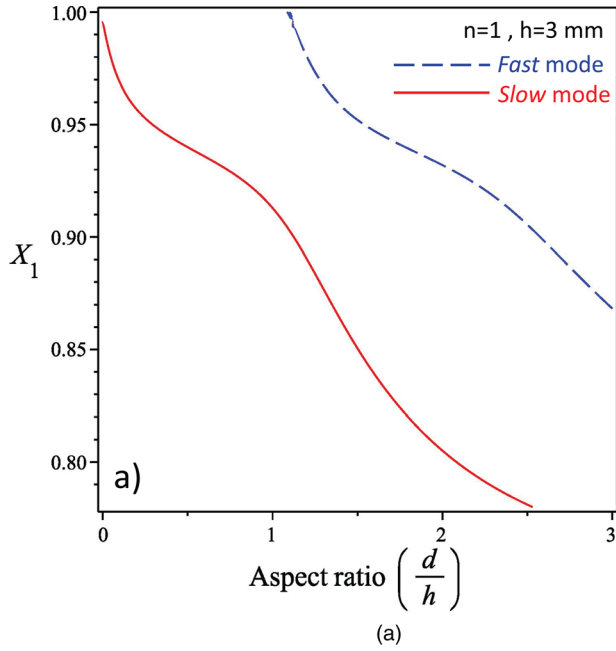


FIG. 5. (Color online) Dimensionless parameter X_n plotted as a function of the aspect ratio d/h for slow and fast modes at different resonances $n = 1$ (a) and $n = 4$ (b).

obtain the following minimal aspect ratio below which the fast mode cannot propagate:

$$\left(\frac{d}{h}\right)_{\min} = \frac{1}{n\pi\sqrt{(c_{1t}/c_f)^2 - 1}} \left\{ \arctan\left(\frac{\rho_f}{\rho_1}\sqrt{\frac{1-(c_{1t}/c_{1l})^2}{(c_{1t}/c_f)^2 - 1}}\right) + \arctan\left[\frac{\rho_f}{\rho_2}\sqrt{\frac{1-(c_{1t}/c_{2l})^2}{(c_{1t}/c_f)^2 - 1}}\right] \times \frac{1}{(2-c_{1t}^2/c_{2t}^2)^2 - 4\sqrt{(1-c_{1t}^2/c_{2t}^2)(1-c_{1t}^2/c_{2l}^2)}} \right\}. \quad (17)$$

Though longitudinally traveling acoustic waves can propagate through any narrow aperture, it follows from Eq. (17) that it is not true for one of the coupled Rayleigh waves. This is because Rayleigh wave, unlike typical acoustic wave, also consists of a transverse component which limits propagation through narrow apertures. For the channel clad between brass and aluminum plates, the first resonance $n = 1$ does not exist if $(d/h) < (d/h)_{\min} = 1.06$. Since in the experiment we always deal with narrow channels with small apertures, $d/h < 1$, we did not observe the cutoff of the fast mode for the primary resonance $n = 1$. However, for the resonance $n = 4$ the critical aspect ratio is 0.26. For this case we observe the cutoff of the fast mode.

The slow mode, unlike the fast one, can propagate in a channel with any small aspect ratio. As shown in Fig. 5 the corresponding value of X does not exceed 1 when $d/h \rightarrow 0$. In a channel with $d/h > (d/h)_{\min}$ the both modes can be excited but if $d/h > (d/h)_{\min}$ it is only the slow mode that transfers acoustic energy from fluid to metal. The cutoff frequency in the spectrum of the fast mode is related to its quasi-symmetric polarization when a maximum in the transverse displacements on one side of the channel occurs at the same coordinate x as a minimum on the other side of the channel. For the slow mode (with quasi-antisymmetric polarization) the maxima and minima occur at the same x .

For the case of identical metals¹⁷ only the symmetric (fast) mode can be excited. Therefore no minima in the transmission spectra were observed for any channel with aspect ratio less than the critical one. In our experiment with different metals we observed minima for the channels with $d/h < (d/h)_{\min}$. Apparently, these minima are due to excitation of the slow mode.

To better understand the transition from slow mode to fast mode in the vicinity of the critical aspect ratio we plot in Fig. 6 the shift of the resonant frequencies with $n = 4$ and $h = 3$ mm with channel aperture d . This plot was obtained

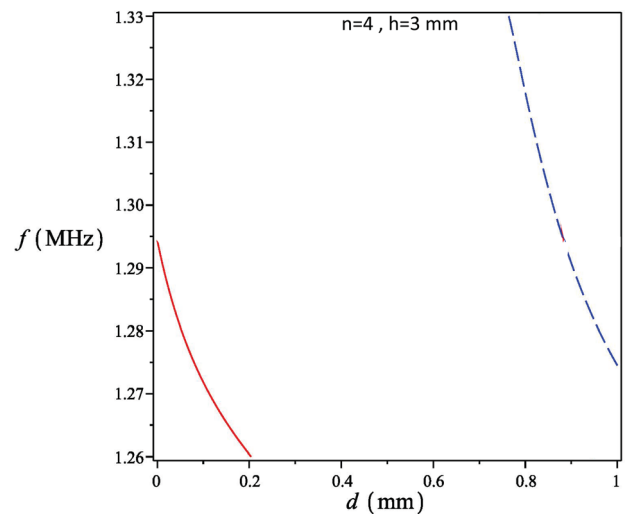


FIG. 6. (Color online) Frequency f versus aperture d of the water channel for slow (solid line) and fast (dashed line) modes obtained using Eq. (15). While the slow mode does not have a critical minimum aperture, the fast mode has a critical minimum aperture at $d = 0.78$ mm. For the case of a water channel clad between identical metal plates, the fast and slow modes become symmetric and antisymmetric modes, respectively, see Ref. 17.

using the dispersion equation (15). It follows from this figure that the transition occurs at $d \approx 0.8$ mm. Around this value one may expect a discontinuous jump due to reduction of frequency when the fast mode is replaced by a slow mode. This jump at $d = 0.75$ mm was indeed observed in the experiment.

Figure 7 shows experimental data for the shift of the resonant frequency with aperture. The shift was obtained from the series of transmission spectra shown in Fig. 2. The frequency of this transition $f \approx 1.34$ MHz is also in a good agreement with the theoretical value of 1.33 MHz.

In the experiment the frequencies of the resonances for the both modes increase as the aspect ratio decreases, in agreement with the theory. This behavior is a direct evidence of the coupling of the Rayleigh waves. Without coupling the frequency should exhibit a tendency to grow with d . This follows from the fact that the phase velocity of a surface mode propagating along a contact of a solid elastic medium with a fluid layer growth with the thickness d of the layer.²⁵

As shown, the resonant frequencies obtained from the experiments and from theoretical calculations are about 91% (at $d = 0.2$ mm) in agreement ($f_{\text{exp}} = 1.38$ MHz, $f_{\text{th}} = 1.26$ MHz) for slow mode and about 95% (at $d = 1$ mm) in agreement ($f_{\text{exp}} = 1.335$ MHz, $f_{\text{th}} = 1.275$ MHz) for fast mode. Hence the close agreement between experiment and theory shows that extraordinary low transmission appears at the resonant frequencies corresponding to the excitation of coupled Rayleigh waves along both surfaces of the water channel. Such a good agreement is observed in spite of the fact that we used approximate boundary condition (14) for quantization of the wave vector. This boundary condition assumes that the Rayleigh waves are completely reflected from at the edges of each plate and a standing wave is formed inside the channel. In real situation there is only a partial reflection at the channel openings. Some part of acoustic energy goes around the corner and the surface wave continues to propagate along the vertical surfaces at the right side in Fig. 1. A numerical method for evaluation of the reflection coefficient

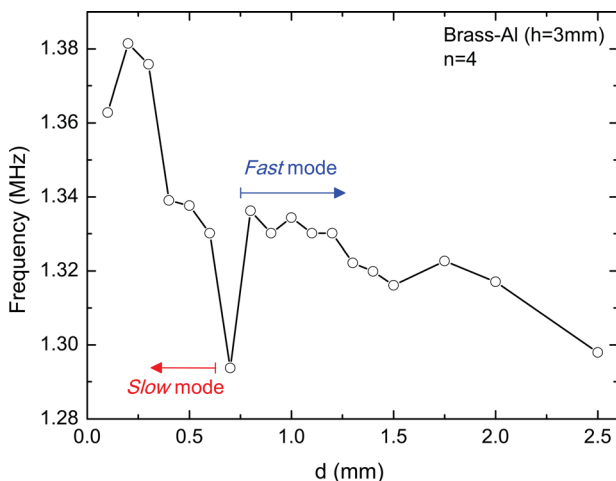


FIG. 7. (Color online) Measured resonant frequencies of the minima of transmission at different apertures d of the water channel. It is clear from the above figure that the fast mode has a critical minimum aperture at around $d_{\text{min}} = 0.75$ mm. On the contrary, the slow mode does not have a critical minimum aperture.

for Rayleigh wave from a right corner was proposed in Ref. 32. It was evaluated that for Rayleigh wave propagating along a metal-vacuum interface the reflection coefficient does not exceed 50%. It, however, may be higher for metal-water interface, due to resonant coupling.

An interesting effect of sound screening in low impedance periodic slit array has been recently predicted in numerical study of the transmission coefficient.³³ This effect is due to diffraction of sound at narrow elastic apertures and it is of non-dissipative nature. Strong reduction of the transmitted sound occurs due to so-called hydrodynamic short circuit when a surface wave excited at the vertical surfaces at the right edge moves in anti-phase with the fluid at the right edge of the slit. In this situation Eq. (14) is not valid at all since pressure at the right end has a negative value instead of zero. The position and the sharpness of the minima caused by the hydrodynamic short circuit strongly depend on the ratio of the impedances of the metal and the fluid. Therefore, it is hard to determine whether some of the deeps in the transmission observed in our experiments are due to hydrodynamic short circuit. There are two minima in Fig. 2, one near 0.7 MHz and another near 1.1 MHz, which cannot be explained by resonant excitation of coupled Rayleigh waves. These minima strongly overlap with Fabry-Perot resonances that makes their analysis more difficult. According to our preliminary data the minimum at 1.1 MHz is due to excitation of leaky Lamb (or Rayleigh) wave. This, however, require further and more detailed study.

VI. POLARIZATIONS OF THE EIGENMODES

In this section we explore the properties of transverse and longitudinal displacements of the metal plates corresponding to different polarizations of coupled Rayleigh waves. Since the displacement vectors of metal plates are expressed in terms of velocity potentials as $\mathbf{w} = \nabla \xi + \nabla \times \mathbf{a}$ for brass ($z > d/2$) and $u = \nabla \phi + \nabla \times \mathbf{b}$ for aluminum ($z < d/2$), their corresponding longitudinal and transverse components are found to be $w_x(x, z) = \partial \xi / \partial x - \partial a / \partial z$, $w_z(x, z) = \partial \xi / \partial z + \partial a / \partial x$ for brass, and $u_x(x, z) = \partial \phi / \partial x - \partial b / \partial z$, $u_z(x, z) = \partial \phi / \partial z + \partial b / \partial x$ for aluminum. Once the relations between the unknown constants in velocity potentials \mathbf{a} , ξ , ϕ , and \mathbf{b} are obtained from a set of homogeneous equations following from the boundary conditions as shown earlier, the displacements turn out to be $u_x, w_x \propto \cos qx$, $u_z, w_z \propto \sin qx$. Although the longitudinal and transverse displacements depend on position x along channel length h , the ratio of longitudinal displacements u_x/w_x and that of the transverse displacements u_z/w_z taken at the metal surfaces are independent of x . In general, for any metal combination, the ratio $u_z/w_z > 0$ for slow mode and $u_z/w_z < 0$ for fast mode. In particular, it can be calculated that for a channel of length $h = 3$ mm and aperture $d = 2.5$ mm, the ratio of the transverse displacements of aluminum to brass $u_z/w_z = -1.3$, and the ratio of the longitudinal displacements $u_x/w_x = 0.91$. These values are in a good agreement with numerical simulation shown in Fig. 8.

The difference in the polarizations of slow and fast mode appears as a phase shift between the vibrations of the

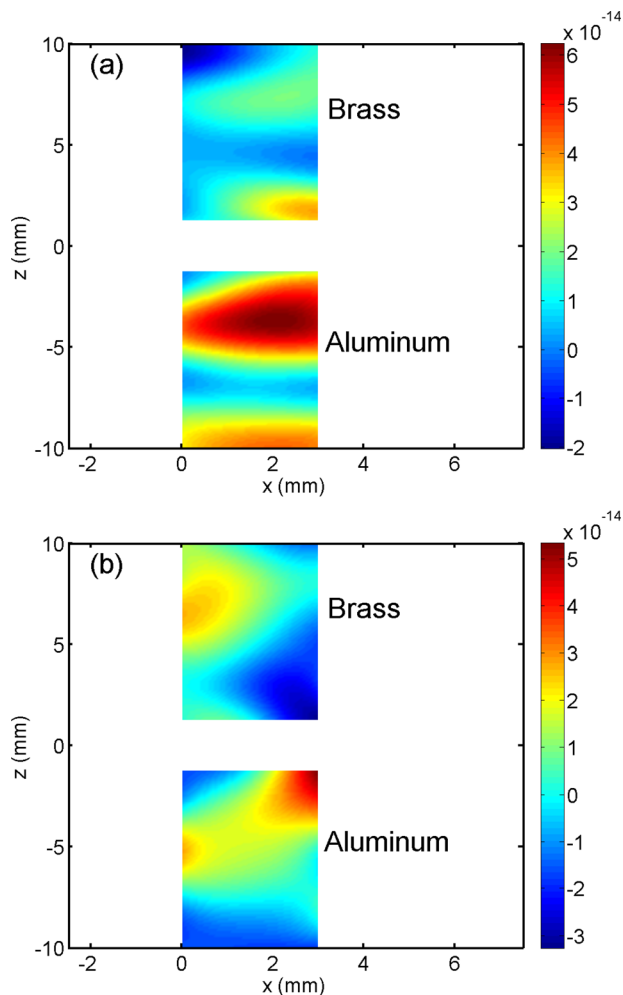


FIG. 8. (Color online) Numerical (COMSOL) simulations for the longitudinal (u_x, w_x) (a) and transverse (u_z, w_z) (b) displacements of the both metal plates induced by propagating plane wave with $f = 368.5$ kHz in water channel with $h = 3$ mm and $d = 2.5$ mm. This frequency corresponds to the first minimum in the transmission spectra in Fig. 2. The ratios of longitudinal to transverse displacements plotted using COMSOL and the theory are in a good agreement.

metal plates. It is easy to demonstrate that the phase shift between the vibrations of the plates is independent of the elastic properties of the plates. However, the relative amplitudes of the displacements (longitudinal, u_x, w_x and transverse, u_z, w_z) change with the type of metals. For the plates of identical metals the amplitudes of longitudinal and transverse vibrations possess the following symmetry: $u_x(x, z) = -w_x(x, -z)$, $u_z(x, z) = w_z(x, -z)$ for slow mode, and $u_x(x, z) = w_x(x, -z)$, $u_z(x, z) = -w_z(x, -z)$ for fast mode. Relating polarization of the mode to the symmetry of its transverse displacement, we conclude that the slow mode is antisymmetric and the fast mode is symmetric. In the case of different metals the symmetry is broken and we refer to the polarizations as being quasi-antisymmetric and quasi-symmetric. At this point it is worthwhile to note that the absence of resonances $n = 2, 3$ in Fig. 2 could be attributed to the fact that the metal plates are fixed in place by sample holder (see Fig. 1). It is possible that the fixation of metal plates by their upper part allows longitudinal and transverse displacements in a way that does not permit certain resonances

to manifest. However, to verify this possibility, it is desirable to carry out further experimental investigation and analysis of the displacements of the center of mass of the metal plates.

VII. CONCLUSION

We have studied extraordinary attenuation of acoustic energy due to resonant excitation of Rayleigh waves in a finite length water channel clad between two unidentical metal plates. We derived the dispersion equation for the channel eigenmodes and calculate the resonant frequencies which coincide with those observed in the experiment. Two eigenmodes with different polarizations and phase velocities are obtained from the dispersion equation. For the case of unidentical metals these modes do not possess definite symmetry (like symmetric and antisymmetric modes for a channel formed by identical metals) and we label them by slow and fast modes. For the fast mode we observe an interesting effect of cutoff at certain critical aperture. This cutoff is unusual for sound wave which penetrates freely through any narrow aperture. Precise measurements of a slight shift of the resonance minima in the transmission spectra with the channel aperture confirm the theoretically predicted effect of coupling and synchronization of the Rayleigh waves. Due to high level of attenuation this effect may be used in designing of metamaterial acoustic screeners. To increase the width of the attenuation band we plan to study similar effect in a set of subwavelength periodic slits. The methods discussed in this paper may also be used in non-destructive testing for layered media.

ACKNOWLEDGMENTS

Work supported by the DOE Grant No. DE-FG02-06ER46312, and by the ONR Grant No. N00014-12-1-0216. A.K. acknowledges the support from the Spanish MEC under Grant No. SAB2009-0006 and the UPV program “Ayda para Estancia de Investigadores de Prestigio.” We thank Ciprian Sarl for technical support. T.L.-R. acknowledges useful discussions with P. Halevi and A. Wirgin.

- ¹P. M. Morse and P. J. Rubenstein, “The diffraction of waves by ribbons and by slits,” *Phys. Rev.* **54**, 895–898 (1938).
- ²H. A. Bethe, “Theory of diffraction by small holes,” *Phys. Rev.* **66**, 163–182 (1944).
- ³A. Sommerfeld, *Optics* (Academic, New York, 1954), pp. 207–246.
- ⁴J. W. Strutt and B. Rayleigh, *The Theory of Sound* (Dover Publications, New York, 1945), pp. 1–480.
- ⁵S. Tinti, “Diffraction by a thick slitted screen,” *J. Acoust. Soc. Am.* **65**, 888–895 (1979).
- ⁶G. P. Wilson and W. W. Soroka, “Approximation to the diffraction of sound by a circular aperture in a rigid wall of finite thickness,” *J. Acoust. Soc. Am.* **37**, 286–297 (1965).
- ⁷A. N. Norris and H. A. Luo, “Acoustic radiation and reflection from a periodically perforated rigid solid,” *J. Acoust. Soc. Am.* **82**, 2113–2122 (1987).
- ⁸B. Hou, J. Mei, M. Ke, W. Wen, Z. Liu, J. Shi, and P. Sheng, “Tuning Fabry–Perot resonances via diffraction evanescent waves,” *Phys. Rev.* **76**, 054303–054308 (2007).
- ⁹T. W. Ebbesen, H. J. Lezec, H. F. Ghaemi, T. Thio, and P. A. Wolff, “Extraordinary optical transmission through sub-wavelength hole arrays,” *Nature* **391**, 667–669 (1998).
- ¹⁰H. F. Ghaemi, Tineke Thio, D. E. Grupp, T. W. Ebbesen, and H. J. Lezec, “Surface plasmons enhance optical transmission through subwavelength holes,” *Phys. Rev.* **58**, 6779–6782 (1998).

- ¹¹M.-H. Lu, X.-K. Liu, L. Feng, J. Li, C.-P. Huang, Y.-F. Chen, Y.-Y. Zhu, S.-N. Zhu, and N.-B. Ming, "Extraordinary acoustic transmission through a 1D grating with very narrow apertures," *Phys. Rev. Lett.* **99**, 174301 (2007); Y. Zhou, M.-H. Lu, L. Feng, X. Ni, Y.-F. Chen, Y.-Y. Zhu, S.-N. Zhu, and N.-B. Ming, "Acoustic surface evanescent wave and its dominant contribution to extraordinary acoustic transmission and collimation of sound," *ibid.* **104**, 164301 (2010).
- ¹²H. Estrada, P. Candelas, A. Uris, F. J. García de Abajo, and F. Meseguer, "Extraordinary sound screening in perforated plates," *Phys. Rev. Lett.* **101**, 084302–084305 (2008).
- ¹³J. Christensen, L. Martín-Moreno, and F. J. García-Vidal, "Enhanced acoustical transmission and beaming effect through a single aperture," *Phys. Rev.* **81**, 174104–174109 (2010).
- ¹⁴H. Estrada, F. J. García de Abajo, P. Candelas, A. Uris, F. Belmar, and F. Meseguer, "Angle-dependent ultrasonic transmission through plates with subwavelength hole arrays," *Phys. Rev. Lett.* **102**, 144301–144304 (2009).
- ¹⁵I. S. Spevak, A. Yu. Nikitin, E. V. Bezuglyi, A. Levchenko, and A. V. Kats, "Resonantly suppressed transmission and anomalously enhanced light absorption in periodically modulated ultrathin metal films," *Phys. Rev.* **79**, 161406–161409 (2009).
- ¹⁶T. M. Slipchenko, D. V. Kadygob, D. Bogdanis, V. A. Yampolskii, and A. A. Krokhin, "Surface and waveguide Josephson plasma waves in slabs of layered superconductors," *Phys. Rev.* **84**, 224512 (2011).
- ¹⁷V. M. García-Chocano, T. Lopez-Rios, A. Krokhin, and J. Sanchez-Dehesa, "Resonant excitation of coupled Rayleigh waves in a short and narrow fluid channel clad between two identical metal plates," *AIP Adv.* **1**, 041501 (2011).
- ¹⁸P. P. Lloyd and M. Redwood, "Wave propagation in a layered plate composed of two solids with perfect contact, slip, or a fluid layer at their interface," *Acustica* **16**, 169–173 (1965).
- ¹⁹P. W. Staecker and W. C. Wang, "Propagation of elastic waves bound to a fluid layer between two solids," *J. Acoust. Soc. Am.* **53**, 65–74 (1973).
- ²⁰W. Hassan and P. B. Nagy, "On the low-frequency oscillation of fluid layer between two elastic plates," *J. Acoust. Soc. Am.* **102**, 3343–3348 (1997).
- ²¹J. Laperre and W. Thys, "Mode coupling in solid/liquid/solid trilayers," *J. Acoust. Soc. Am.* **96**, 1643–1650 (1994).
- ²²O. Lenoir, J.-L. Izbicki, M. Rousseau, and F. Coulouvrat, "Subwavelength ultrasonic measurement of a very thin fluid layer thickness in a trilayer," *Ultrasonics* **35**, 509–515 (1997).
- ²³J. Christensen, L. Martín-Moreno, and F. J. García-Vidal, "Theory of resonant acoustic transmission through subwavelength apertures," *Phys. Rev. Lett.* **101**, 014301–014304 (2008).
- ²⁴Z. Liang and J. Li, "Extreme acoustic metamaterial by coiling up space," *Phys. Rev. Lett.* **108**, 114301 (2012).
- ²⁵I. A. Viktorov, *Rayleigh and Lamb Waves* (Plenum, New York, 1967), Chap. 1.
- ²⁶L. D. Landau and E. M. Lifshitz, *Fluid Mechanics*, 2nd ed. (Butterworth-Heinemann, London, 1987), pp. 1–552.
- ²⁷An eigenmode propagating slower than sound in fluid has been predicted in Ref. **19**.
- ²⁸C. T. Schröder and W. R. Scott, Jr., "On the complex conjugate roots of the Rayleigh equation: The leaky surface wave," *J. Acoust. Soc. Am.* **110**, 2867–2877 (2001).
- ²⁹N. E. Glass and A. A. Maradudin, "Leaky surface-elastic waves on both flat and strongly corrugated surfaces for isotropic, nondissipative media," *J. Appl. Phys.* **54**, 796–805 (1983).
- ³⁰E. Smith, P. S. Wilson, F. W. Bacon, J. F. Manning, J. A. Behrens, and T. G. Muir, "Measurement and localization of interface wave reflections from a buried target," *J. Acoust. Soc. Am.* **103**, 2333–2343 (1998).
- ³¹Q. Qi, "Attenuated leaky Rayleigh waves," *J. Acoust. Soc. Am.* **95**, 3222–3231 (1994).
- ³²A. K. Gautesen, "Scattering of a Rayleigh wave by an elastic quarter space revisited," *Wave Motion* **35**, 91–98 (2002).
- ³³H. Estrada, J. M. Bravo, and F. Meseguer, "High sound screening in low impedance slit arrays," *New J. Phys.* **13**, 043009 (2011).